May 2007

Role of thermodynamic fluctuations in magnetic recording (invited)

Ralph Skomski
University of Nebraska-Lincoln, rskomski2@unl.edu

Role of thermodynamic fluctuations in magnetic recording (invited)

Ralph Skomski[a)]
Department of Physics and Astronomy, University of Nebraska, Lincoln, Nebraska 68588
and Nebraska Center for Materials and Nanoscience, University of Nebraska, Lincoln, Nebraska 68588

(Presented on 9 January 2007; received 3 November 2006; accepted 30 January 2007; published online 8 May 2007)

The thermal stability of the information stored in magnetic recording media is determined by a complex hierarchy. The leading consideration is the static or zero-temperature magnetization reversal complemented by the intrinsic temperature dependence of the micromagnetic parameters. Thermally activated Arrhenius (or Néel-Brown) processes modify the reversal by realizing paths close to static reversal, whereas "giant fluctuations" corresponding to reversal fields much higher than the nucleation field can safely be excluded. Thermally activated reversal in very thin elongated nanoparticles limits the thermal stability of magnetic recording media but degenerates into coherent rotation as the temperature is lowered, thereby reconciling micromagnetism and thermodynamics. A particularly complicated situation is encountered in alloys, where sublattices containing heavy transition-metal atoms act like earthquakes that modify the energy landscape. © *2007 American Institute of Physics*. [DOI: 10.1063/1.2714322]

I. INTRODUCTION

Thermally activated magnetization reversal is a key consideration in ultrahigh-density magnetic recording, because the ever-decreasing bit and particle size facilitate thermally activated magnetization reversal.[1–3] In a simple picture, the magnetization of particles of volume V and uniaxial anisotropy K_1 is stabilized by an energy barrier K_1V, and when V is very small, then the room-temperature magnetization direction becomes unstable due to thermal activation. The decay of the magnetization is a manifestation of the magnetic aftereffect, which was discovered as early as 1889.[4]

If K_1V was the only consideration, then one could achieve virtually diverging areal densities by using long cylinders of volume $V=\pi R^2L$, where R and h are the radius and the length (height) of the cylinders. The closely related and exactly solvable micromagnetic case of long ellipsoids of revolution[5] indicates that the coercivity remains finite as R approaches zero. In a strict sense, this finding is limited to zero temperature, but analyzing the involved Boltzmann factors reveals that the same is true for nonzero but low temperatures.[6]

However, the finite coercivity predicted by micromagnetic analysis is at odds with the findings of statistical mechanics, which predicts the absence of ferromagnetism in one-dimensional magnets, including infinite wires.[7,8] The situation is complicated by the well-known experimental findings that magnetization reversal in nanowires involves volumes much *smaller* than the wire volume[9] and that coercivities are often much lower than predicted from the above-mentioned micromagnetic nucleation modes. Micromagnetism explains the low coercivities and small activation volumes by structural imperfections,[5,6] whereas the finite-temperature approach assumes thermal activation.[7,8] If the thermal mechanism was the main consideration, then the finite-temperature behavior would be quite different from the zero-temperature limit. This is not observed—typical activation volumes and the coercivities remain small at zero temperature and can be traced to structural imperfections.

The aim of this paper is to reconcile the seemingly contradictory thermodynamic and micromagnetic approaches and to elaborate how magnetization reversal is realized in magnetic particles of interest in magnetic recording. We will see and analyze that the reversal obeys a complicated hierarchy. First, static magnetization processes are largely determined by imperfections and dominate at low temperature. As a crude rule, static magnetization reversal in particles smaller than 5 nm is coherent, whereas larger particles tend to reverse incoherently, by a variety of different mechanisms (Sec. II). Second, the intrinsic temperature dependences of micromagnetic parameters, such as the spontaneous magnetization M_s and anisotropy K_1, modify the static behavior (Sec. III). Third, there are corrections due to Arrhenius- or Néel-Brown-type thermal activation over static energy barriers (Sec. IV). Fourth, "giant" thermodynamic fluctuations may lead to reversal paths other than that corresponding to static reversal, or modify the energy landscape.

Throughout the paper, emphasis is on temperatures significantly below the Curie temperature T_C, excluding critical fluctuations and very fast phenomena.[10,11] The latter are important for heat-assisted magnetic recording[3] but irrelevant for the long-term stability of stored information.

II. STATIC REVERSAL

Finite-temperature magnetization reversal is almost always based on *static* magnetization reversal, which implies the vanishing of a metastable energy minimum in a reverse magnetic field. This section summarizes typical mechanisms.

A widely known coercivity mechanism is the Stoner-Wohlfarth (SW) reversal or coherent rotation, but there are other well-investigated and important mechanisms. A key

[a)]Electronic mail: rskomski@neb.rr.com

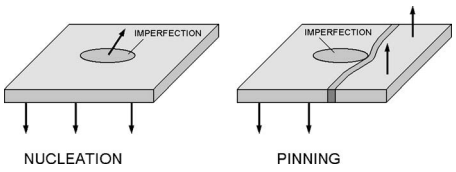

FIG. 1. Static magnetization reversal: (i) nucleation and (ii) pinning. There are many subcategories, such as delocalized nucleation (coherent rotation and curling), Kersten and Gaunt-Friedel strong-pinning mechanisms, weak pinning, and various intermediate mechanism involving ensembles of interacting grains or particles.

distinction is between nucleation and pinning (Fig. 1). Nucleation is defined as the instability of a magnetization state in a reverse field. Figure 2 illustrates that there are three basic types of nucleation, (a) coherent rotation, (b) curling, and (c) localized nucleation. For coherent rotation and curling, the respective nucleation fields (coercivities) are

$$H_c = \frac{2K_1}{\mu_0 M_s} + \frac{1}{2}(3D-1)M_s \tag{1}$$

and

$$H_c = \frac{2K_1}{\mu_0 M_s} - DM_s + \frac{c(D)A}{\mu_0 M_s R^2}. \tag{2}$$

In the latter equation, c is 8.666 for spheres ($D=1/3$) and 6.678 for needles ($D=0$),[5,12] whereas the hemisphere model of Fig. 2 is described by $D=1/3$ and $c=8$.[13]

Curling costs exchange energy but is magnetostatically favorable due to vortexlike flux closure. In perfect ellipsoids of revolution, there is a transition from coherent rotation to curling for radii larger than about 10 nm.[5,6] This transition is independent of the anisotropy and unrelated to the single-domain character of the magnet—many or most particles in permanent magnetism and high-density magnetic recording are single domain but reverse incoherently, with a relatively low coercivity.[6] Aside from curling effects, this reflects *localized nucleation* due to "soft" imperfections.[6,14] An exception are particles smaller than about 5 nm, where reversal is coherent (Stoner-Wohlfarth-like), irrespective of the presence of imperfections and grain boundaries.

Pinning means that imperfections impede the motion of preexisting domain walls and dominates the behavior in strongly disordered magnets. Weak pinning is frequently encountered in soft magnetic materials and refers to the trapping of a wall by ensembles of many pinning centers, whereas strong pinning is realized by a few relatively strong defects, as in Fig. 1. Depending on the domain-wall curvature, one encounters Kersten pinning,[15] where the coercivity

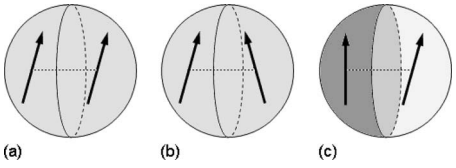

FIG. 2. Static nucleation modes in a hemisphere model: (a) coherent rotation, (b) curling, and (c) localized nucleation. In magnetic recording, very small particles ($R<5$ nm) reverse coherently, whereas large particles experience localized nucleation.

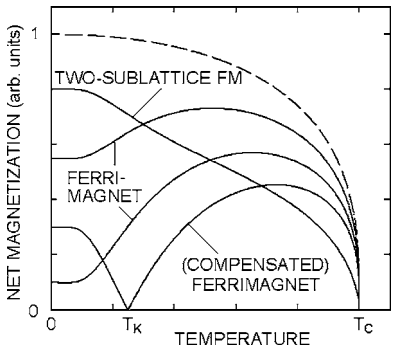

FIG. 3. Temperature dependence of the magnetization of ferro- and ferrimagnets. T_K is a ferromagnetic compensation point. These scenarios are frequently encountered in rare-earth transition-metal compounds. The dashed line is a simple ferromagnet.

H_c is proportional to the pinning force p,[15] or Gaunt-Friedel pinning, where $H_c \sim p^2$.[16] In thin films, the latter relation changes to $H_c \sim p^{3/2}$. In a very broad sense, pinning includes interacting particles[17] and particulate recording media, where the domain walls are located between interacting particles.[18]

III. INTRINSIC TEMPERATURE DEPENDENCE

The next consideration in our hierarchy is the temperature dependence of intrinsic magnetic properties. In other words, atomic-scale equilibrium fluctuations responsible for $M_s(T)$ and $K_1(T)$ determine the temperature dependence of anisotropy and coercivity. This effect is often much larger than thermally activated jumps over energy barriers, but it is time independent and easily incorporated into micromagnetic calculations.

An interesting aspect of finite-temperature anisotropy is the involvement of interatomic exchange. In $L1_0$ magnets such as PtCo, the anisotropy energy per atom corresponds to a temperature equivalent to only 4.3 K, and the temperature dependence of the anisotropy of magnetic alloys is actually determined by *interatomic exchange*. A complicating feature is that highly anisotropic materials, such as the $L1_0$ alloys, contain two or more magnetic sublattices[19] with different and generally strongly temperature-dependent anisotropies. Sublattice effects such as ferrimagnetic compensation (Fig. 3) may be exploited in heat-assisted magnetic recording (HAMR).

Figure 4 shows the temperature dependence of the *magnetic anisotropy*, which is largely determined by the intersu-

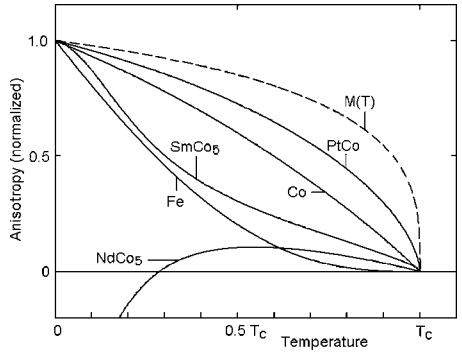

FIG. 4. Temperature dependence of the anisotropy (schematic).

blattice exchange J^* and generally more pronounced than the temperature dependence of the magnetization. Simple ferromagnets, such as Fe and Co, are well described by the Callen and Callen model,[20] which goes back to Akulov.[21] The model predicts power laws of the type $K(T) \sim M_s(T)^m$, where nth order anisotropy constants obey $m=n(n+1)/2$. For example, K_1 is characterized by the power-law exponents $m=3$ (uniaxial) and $m=10$ (cubic).

The Callen and Callen approach is a poor approximation for alloys, because it relates the anisotropy to the net magnetization, rather than taking into account that the main anisotropy contribution comes from heavy atoms ($4d$, $5d$, or $4f$ electron), whereas the magnetization is largely due to the $3d$ elements. For example, rare-earth anisotropy reflects the electrostatic crystal-field interaction of the aspherical $4f$ charge clouds. Thermal intramultiplet excitations ($-J \leqslant J_z \leqslant J$) destroy the net asphercity of the $4f$ charge clouds by randomizing the directions of the rare-earth moment and result in the complicated net anisotropy.[22] Other compounds have deviating second-order exponents, such as $m=2$ for $L1_0$ magnets and $m=1$ for actinide compounds.[23] In $L1_0$ magnets, the temperature dependence of the anisotropy is linked to the collapse of the $4d/5d$ moment.[24,25] In all cases, the anisotropy is of the single ion type, as contrasted to Néel-type pair anisotropy.

IV. MAGNETIZATION DYNAMICS

A key aim of the paper is to rationalize the temperature dependence of the magnetization. It is possible to predict the evolution of any physical system from the time-dependent Schrödinger equation $i\hbar\partial|\Psi\rangle/\partial t=\mathsf{H}|\Psi\rangle$, but in most cases this is neither practical nor necessary. *Coarse-grained equations* abstract from irrelevant heat-bath degrees of freedom and focus on relevant degrees of freedom, such as domain-wall positions. Important examples are master or rate equations, Fokker-Planck equations, and Langevin (or random-force) equations, which are physically largely equivalent.[26,27] These equations form the basis for the following sections and are therefore briefly explained.

The introduction of transition rates $W(s,s')=W(s' \rightarrow s)$ between states s' and s yields the rate or master equation

$$\frac{\partial P(s)}{\partial t} = \int [W(s,s')P(s') - W(s',s)P(s)]ds' \tag{3}$$

for the probability $P(s)$. Assuming random but small jumps $\pm\Delta s$ (diffusion) and a deterministic term (drift) yields the Fokker-Planck equation

$$\frac{\partial P}{\partial t} = \frac{\Gamma_0}{k_BT}\frac{\partial}{\partial s}\left(\frac{\partial E}{\partial s}P\right) + \Gamma_0\frac{\partial P^2}{\partial s^2}, \tag{4}$$

where the drift is described by the force $\partial E/\partial s$. In some cases, it is possible to find exact solutions. For example, the zero-field magnetization of small platelike particles with zero in-plane anisotropy decays as $M_x(t)=M_x(0)\ \exp(-\Gamma_0 t)$.[28] In the limit of nonequilibrium states captured in deep potential valleys (activation energy $E_a \gg k_BT$), the Focker-Planck dynamics approaches the Arrhenius limit with the relaxation rate $\Gamma_0 \exp(-E_a/k_BT)$. This regime is also known as Kramers' escape-rate theory[29] and, in magnetism, as the Arrhenius-Néel-Brown theory. The Landau-Lifshitz precession enters these expressions only indirectly by affecting Γ_0.

Solving the Fokker-Planck equation yields the probability $P(s,t)$, from which averages such as $\langle s(t)\rangle$ and $\langle s(t)s(t')\rangle$ are obtained by integration. The explicit calculation of $P(s)$ can be avoided by using the *Langevin equation*

$$\frac{\partial s}{\partial t} = -\frac{\Gamma_0}{k_BT}\frac{\partial E}{\partial s} + \sqrt{2\Gamma_0}\xi(t). \tag{5}$$

Here the random thermal forces $\xi(t)$ have the character of a delta-correlated white noise, where $\langle\xi(t)\rangle=0$ and $\langle\xi(t)\xi(t')\rangle = \delta(t-t')$ ensure the equilibrium limit $P \sim \exp(-E/k_BT)$.

Kramers' escape-rate theory yields the above-introduced Arrhenius or Néel-Brown law, which has been used in magnetism since the 1930s,[30]

$$\tau = \tau_0 \exp\left(\frac{E_a}{k_BT}\right), \tag{6}$$

where E_a is the activation energy associated with the energy barrier and $\tau_0=1/\Gamma_0$ is an inverse attempt frequency of the order of 10^{-10}–10^{-9} s. There is also an activation *entropy* S_a describing the number of paths over the energy barrier, so that $\tau=\tau_0 \exp[(E_a-TS_a)/k_BT]$, but S_a is conveniently incorporated into τ_0.[31] In Kramers' theory, S_a increases with decreasing curvature of the energy maximum (saddle point).

Inverting Eq. (6) and assuming a time scale $\tau \sim 100$ s yields the accessible energy barrier $E_a=k_BT\ln(\tau/\tau_0)$, or $E_a=25k_BT$. This is the well-known 25-kT rule. At room temperature, the surmountable energy barrier is therefore $E_a/k_B=7500$ K, significantly smaller than typical micromagnetic energy barriers of the order of 100 000 K. In magnetic recording, $\tau \sim 10y$, and the corresponding energy barrier $E_a \geqslant 40k_BT$ (up to $70k_BT$ for high reliability).

A slightly different equation is the logarithmic *magnetic-viscosity* law

$$M(H,t) = M(H,t_0) - S\ln(t/t_0), \tag{7}$$

where S is the magnetic-viscosity constant.[9,22,30] For example, typical permanent magnets lose a small fraction of their magnetization, typically a few 0.1%, within the first hours after production. This Jordan aftereffect is due to energy-barrier distributions naturally occurring in magnetic materials[30] and reproduced by integration over all energy barriers,

$$M(t) = -M_s + 2M_s\int_{-\infty}^{\infty} P(E)e^{-\Gamma_0 t\ \exp(-E/k_BT)}dE. \tag{8}$$

For low temperatures, this yields $M(t)=M(t_0) - 2M_sk_BTP(E_0)\ln(t/t_0)$.

Figure 5 shows that the energy in Eq. (6) depends on the magnetic field. A frequently used energy-barrier expression is

$$E_a = K_0V_0\left(1-\frac{H}{H_0}\right)^m, \tag{9}$$

where parameters K_0, V_0, H_0, and m describe the magnet's real structure. Zero-temperature or static switching occurs

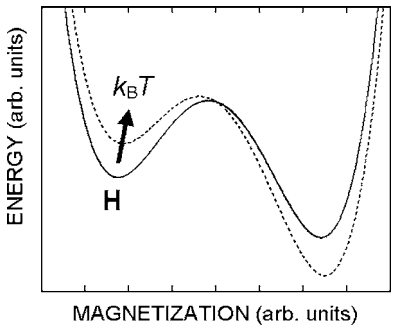

FIG. 5. Field induced and thermally activated magnetization processes. In most systems, thermal activation is a small correction to the leading field-dependent or "static" mechanism.

when E_a vanishes, that is, for $H=H_0$. Substituting E_a into Eq. (6) and equating the field H with H_c yields the Kneller-Sharrock equation[38]

$$H_c = H_0\left\{1 - \left[\frac{k_BT}{K_0V_0}\ln(\tau/\tau_0)\right]^{1/m}\right\}. \tag{10}$$

Equations (9) and (10) mean that thermally activated reversal is facilitated by an external field which reduces E_a until the static switching condition $H=H_0$ is nearly satisfied (Fig. 5). Note that K_0 and $H_0 \sim 2K_0/M_s$ are both temperature dependent (Sec. III).

To derive m in Eq. (9), one expands the micromagnetic energy in the vicinity of the saddle point. The inclusion of linear, quadratic, and cubic terms yields $m=3/2$. This exponent was first obtained by Néel in 1950 and describes a variety of coherent and incoherent magnetization processes, such as strong domain-wall pinning and the reversal of misaligned Stoner-Wohlfarth particles.[6,16,32,33] For symmetric energy barriers, the cubic coefficient is zero, and one must include a quartic term. This changes the exponent to $m=2$, as exemplified by aligned Stoner-Wohlfarth particles.

Linear laws ($m=1$) are occasionally assumed in calculations, but their derivation from physically meaningful energy landscapes has remained elusive.[33] Other approaches start from unrealistic or ill-defined energy landscapes. For example, series expansion in the vicinity of H_0 reduces $E_a \sim (1/H-1/H_0)$ to an $m=1$ law, but for $H=0$ it amounts to the unphysical prediction of an infinite energy barrier. Note that linear laws $E_a \sim H_0-H$ looks like a Zeeman energy, but the Zeeman interaction does *not* lead to a linear field dependence.[23] However, linear laws can be used to rationalize experimental data,[9] using $E_a \sim M_sV^*(H-H_0)$ to derive temperature-dependent activation volumes V^*.[22,31]

V. CASE STUDY: COMPOSITE NANOPARTICLES

Before returning to our original problem of reconciling thermodynamics and micromagnetics, let us use an example to summarize Secs. II–IV. In magnetic recording, one tries to combine writability (small H_c) with thermal stability (large E_a). One possible scenario is to exchange couple hard and soft regions.[34–37] In the simplest case one considers a hard particle of volume V_0 and anisotropy $K(T)$ coupled to soft particle of volume V_0 and zero anisotropy. The total energy is

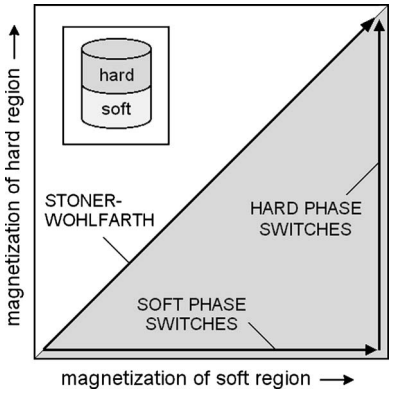

FIG. 6. Static phase diagram for coupled hard and soft regions. In this figure, the original magnetization state is $\downarrow$ ($\cos\theta_h=\cos\theta_s=-1$) and the applied field points in the $\uparrow$ direction. The inset shows a typical geometry.

$$E = -J\cos(\theta_h-\theta_s) - KV_0\cos^2\theta_h - \mu_0M_sHV_0(\cos\theta_h + \cos\theta_s). \tag{11}$$

Here J is the effective exchange coupling between the particles defined[6] as a volume integral over the interface region between the particles.

Figure 6 shows the $\cos\theta_h$-$\cos\theta_s$ plane and illustrates two limits:[39] (i) SW reversal ($\theta_h=\theta_s$) for large J and (ii) localized reversal, where the soft phase switches first, for $J<KV_0$. The coercivities are K/μ_0M_s (SW) and $(2K-J/V_0)/\mu_0M_s$ (localized), whereas the zero-field energy barriers remains KV_0 (SW), as contrasted to $KV_0(1+J/2KV_0)^2$ (localized).

The reduced coercivity causes the ratio E_a/H_c to increase by a factor of $1/(1-J/2K_0V_0)$, and the corresponding quality factor of $2E_a/\mu_0M_sV$ varies between the SW value 1 ($J=0$) and 2 ($J=KV_0$). However, E_a and H_c have different units, and the quality factor involves the *subsystem* volume V_0. One might equally well use the total volume $V=2V_0$, so that the quality factor decreases by a factor of 2 and not exceeds the SW value of 1 corresponding to strong exchange coupling.

Elongated particles with a continuous anisotropy gradient $K_1(z)$, which may be achieved by multilayering[37] or by chemical concentration gradients, yield a coercivity reduction of order δ_B/h, where h is the length of the particle and δ_B is the Bloch-wall width. The particle volume $V=hA_0$, where A_0 is the cross-section area of the particle, provides a natural choice to fix E_a/H_c. The areal density, determined by A_0, is independent of the "idle" parameter h, but in Sec. VI we will see that h affects the thermal stability. Thin and long particles tend to be magnetically unstable, especially in the presence of soft regions (small K_1). Furthermore, the control of the domain-wall motion in the middle of elongated wires is difficult and effectively limits the areal density.

VI. GIANT FLUCTUATIONS

At zero temperature, the magnetization reversal is realized by the path with the lowest saddle-point energy. "Giant fluctuations," which are reminiscent of the thermally activated uphill motion of a big stone, have very small Boltzmann factors $\exp(-E_a/k_BT)$ and can usually be ignored.

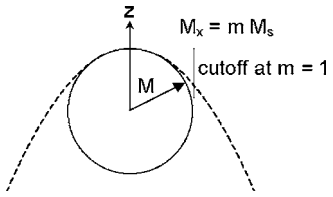

FIG. 7. Harmonic approximation and magnetization cutoff.

However, the activation energy for small particles is K_1V, and for sufficiently small particles, E_a become comparable to k_BT. The same is true for thin wires of radius R, where the activation energy scales as πR^2. This makes long and thin wires unsuitable for data storage.

To reconcile statistical mechanics[7,8] and micromagnetism,[5,6] we use a harmonic approximation. Figure 7 shows that the approximation breaks down when the magnetization angle reaches 90° ($M_x=M_s$). This provides a natural cutoff for the perpendicular magnetization component $m=M_x/M_s$, and the Langevin equation reduces to

$$\frac{\partial m(\mathbf{r})}{\partial t} = [2A\nabla^2 m - (2K - \mu_0 H M_s)m]V + \sqrt{2\Gamma_0}\xi(\mathbf{r},t). \tag{12}$$

It is easily solved by normal-mode analysis and yields both the lowest lying mode (nucleation mode) and excited modes, including giant fluctuations.

Figure 8 shows the considered geometries. We assume that the spin in the center of the nucleus has a magnetization angle of 90° and that the mode decays exponentially with a field-dependent decay length L. This yields the energy

$$E = A_d\left(\sqrt{\frac{\pi}{d}}L\right)^d\left[A\frac{d^2}{2L^2} + \left(K - \frac{1}{2}\mu_0 M_s H\right)\right], \tag{13}$$

where $A_d \sim R^{3-d}$. Figure 9 shows the energy of the zero-field fluctuations as a function of the fluctuation size. The physical realization of the modes is governed by their Boltzmann factors.

In *one dimension*, the energy depends on the radius of the wire. A rough but essentially correct argument is to assume that thermal activation leads to the reversal of a wire segment of length $2L$. This is paid by the creation of two domain walls of combined energy $2\pi R^2\gamma$, where $\gamma = 4(AK_1)^{1/2}$ is the domain-wall energy. Equating this energy to $25k_BT$ yields the transition temperature

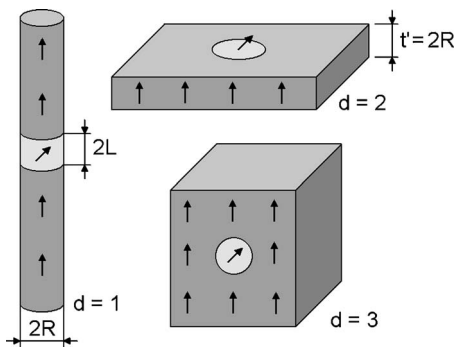

FIG. 8. Geometries for which giant fluctuations are considered.

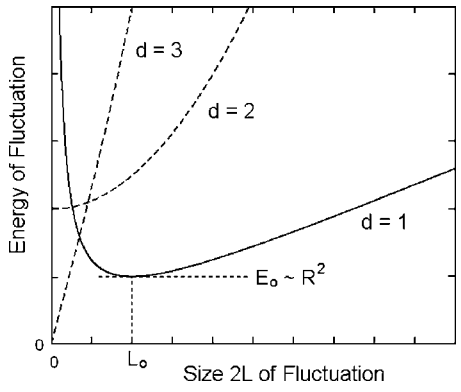

FIG. 9. Energy of zero-field fluctuations as a function of fluctuation size.

$$T_0 = \frac{8\pi R^2\sqrt{AK_1}}{25k_B}, \tag{14}$$

above which giant fluctuations destroy the magnetization on a time scale of 100 s (cf. Sec. IV). For typical ferromagnetic materials with $A=10$ pJ/m and anisotropies of 0.1 and 10 MJ/m^3, the room-temperature stability radii are 4.0 and 1.3 nm, respectively. Equating the Stoner-Wohlfarth expression K_1V with $\pi R^2\gamma$ yields a maximum length for particles of fixed volume, $4(AK_1)^{1/2}=4\delta_B/\pi$. For longer particles, domain-wall creation is more favorable than the Stoner-Wohlfarth rotation. The corresponding energy barrier $4\pi R^2(AK_1)^{1/2}$, rather than $4\pi R^3K_1/3=K_1V$, translates into a maximum recording density of order γ/k_BT.

Below T_0, thermal excitations lead to magnetization fluctuations whose range L is larger than the domain-wall thickness parameter $\delta_0=(A/K_1)^{1/2}$. This is basically a random-field problem[40] and yields

$$L = \frac{\delta_0}{\sqrt{1 - H/H_0}}. \tag{15}$$

In the limit of static magnetization reversal, where $H=H_0$, this equation reproduces the coherent-rotation mode ($L=\infty$). At small temperatures, the fluctuations obey $L\sim 1/T$. This reconciles the dynamic behavior with exact nucleation mode.

In two and especially three dimensions it is easy to form small nuclei (Fig. 9), but they rapidly collapse and do not lead to magnetization reversal. In two dimensions, one obtains the field-independent activation energy $E_a \approx 2\pi At'$, where t' is the film thickness. This energy corresponds to a cylindrical domain of length t' and radius $L\approx 2\delta_0$. Taking $E_a=25k_BT$ and $A=10$ pJ/m, we a obtain room-temperature stability thickness of about 1.5 nm.

VII. SUBLATTICE INSTABILITY

Finally, we briefly discuss giant fluctuations related to anisotropy, as contrasted to magnetization fluctuations. For simplicity, we consider rare-earth fluctuations, Fig. 10(a), in a nanoparticle containing N atoms. Here $K_1(T)\sim K_0J^{*2}/T^2$,[41] and the average anisotropy energy is NK_0J^{*2}/T^2, but fluctuations $\langle K_1^2\rangle - \langle K_1\rangle^2$ play an important role on a local scale. In some regions, the anisotropy is temporarily reduced, similar to the soft region in Fig. 6. This deteriorates the thermal

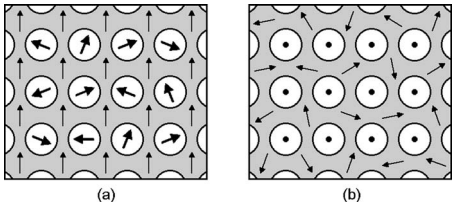

FIG. 10. Exchange and anisotropy: finite-temperature spin structure in (a) RE-TM intermetallics and (b) $L1_0$ magnets. The heavy atoms (white) are embedded in a transition-metal environment (gray). Both mechanisms yield strong deviations from the Callen and Callen picture.

stability of the stored information. Pictorially, thermal activation does not push the magnetization over the saddle point but changes that height of the mountain range, like an earthquake.

The effect can be quite strong. The local random field exerted by the spins in Fig. 10(a) is of order J^*. For a small particle containing N particles, the magnitude of the effect is $N^{1/2}J^*$, and the ratio $\delta E/\langle E\rangle \sim T^2/J^*K_0N^{1/2}$. When δE exceeds $\langle E\rangle$, the fluctuations actually dominate the average anisotropy. This is the case for particles smaller than $N_c \sim T^4/J^{*2}K_0{}^2$. Since $T/K_0 \sim 100$ and $T/J^* \geqslant 1$, $N_c \sim 10\,000$, corresponding to particle diameters of a few nanometers. This example shows that sublattice effects yield a disproportionally strong contribution to the thermal instability.

VIII. CONCLUSIONS

In summary, we have analyzed how thermal excitations affect the magnetization of magnetically stored information. Thermal activation is embedded in a complicated hierarchy involving static magnetization reversal, intrinsic temperature variations, thermal activation over static energy barriers, and giant fluctuations away from static reversal. The static reversal mode is a solution of a well-defined micromagnetic problem. It usually involves structural imperfections and cannot be postulated on intuitive grounds. In a strict sense, there are no giant fluctuations in magnetism, and even extreme cases, such as thin wires, approach the correct micromagnetic limit at low temperatures. However, these excitations have a big impact on the magnetization reversal for extremely high densities, corresponding to bit sizes of about 2 nm. In this regime, the achievable areal density scales as the ratio of domain-wall energy to temperature.

ACKNOWLEDGMENTS

This work is supported by NSF-MRSEC, INSIC, DOE, and NCMN. Thanks are due to D. J. Sellmyer and O. N. Mryasov for stimulating discussions and to V. Skomski for help during the preparation of the manuscript.

[1] D. Weller, A. Moser, L. Folks, M. E. Best, W. Lee, M. F. Toney, M. Schwickert, J.-U. Thiele, and M. F. Doerner, IEEE Trans. Magn. **36**, 10 (2000).
[2] R. L. Comstock, *Introduction to Magnetism and Magnetic Recording* (Wiley, New York, 1999).
[3] D. Weller and T. McDaniel, in *Advanced Magnetic Nanostructures*, edited by D. J. Sellmyer and R. Skomski (Springer, Berlin, 2006), p. 295.
[4] J. A. Ewing, Proc. R. Soc. London **46**, 269 (1889).
[5] A. Aharoni, *Introduction to the Theory of Ferromagnetism* (University Press, Oxford, 1996).
[6] R. Skomski, J. Phys.: Condens. Matter **15**, R841 (2003).
[7] H.-B. Braun and H. N. Bertram, J. Appl. Phys. **75**, 4609 (1994).
[8] H.-B. Braun, J. Appl. Phys. **99**, 08P908 (2006).
[9] D. Givord and M. F. Rossignol, in *Rare-earth Iron Permanent Magnets*, edited by J. M. D. Coey (University Press, Oxford, 1996), p. 218.
[10] U. Nowak, O. N. Mryasov, R. Wieser, K. Guslienko, and R. W. Chantrell, Phys. Rev. B **72**, 172410 (2005).
[11] H. Kachkachi and D. A. Garanin, Physica A **291**, 485 (2001).
[12] W. F. Brown, *Micromagnetics* (Wiley, New York, 1963).
[13] R. Skomski, *Simple Models of Magnetism* (University Press, Oxford, 2007).
[14] R. Skomski and J. M. D. Coey, Phys. Rev. B **48**, 15812 (1993).
[15] M. Kersten, Z. Phys. **44**, 63 (1943).
[16] P. Gaunt, Philos. Mag. B **48**, 261 (1983).
[17] W.-J. Chen, Sh.-F. Zhang, and H. N. Bertram, J. Appl. Phys. **71**, 5579 (1992).
[18] J. Zhou, A. Kashyap, Y. Liu, R. Skomski, and D. J. Sellmyer, IEEE Trans. Magn. **40**, 2940 (2004).
[19] J. S. Smart, *Effective Field Theories of Magnetism* (Sunders, Philadephia, 1966).
[20] H. R. Callen and E. Callen, J. Phys. Chem. Solids **27**, 1271 (1966).
[21] N. Akulov, Z. Phys. **100**, 197 (1936).
[22] R. Skomski and J. M. D. Coey, *Permanent Magnetism* (Institute of Physics, Bristol, 1999).
[23] R. Skomski, O. N. Mryasov, J. Zhou, and D. J. Sellmyer, J. Appl. Phys. **99**, 08E916 (2006).
[24] R. Skomski, A. Kashyap, and D. J. Sellmyer, IEEE Trans. Magn. **39**, 2917 (2003).
[25] O. N. Mryasov, U. Nowak, K. Y. Guslienko, and R. W. Chantrell, Europhys. Lett. **69**, 805 (2005).
[26] H. Risken, *The Fokker-Planck Equation* (Springer, Berlin, 1989).
[27] K.-H. Fischer and A. J. Hertz, *Spin Glasses* (University Press, Cambridge, 1991).
[28] R. Skomski, J. Zhou, and D. J. Sellmyer, J. Appl. Phys. **97**, 10A702 (2005).
[29] H. A. Kramers, Physica (Utrecht) **7**, 284 (1940).
[30] R. Becker and W. Döring, *Ferromagnetismus* (Springer, Berlin, 1939).
[31] R. Skomski, R. D. Kirby, and D. J. Sellmyer, J. Appl. Phys. **85**, 5069 (1999).
[32] R. H. Victora, Phys. Rev. Lett. **63**, 457 (1989).
[33] R. Skomski, J. Zhou, R. D. Kirby, and D. J. Sellmyer, J. Appl. Phys. **99**, 08B906 (2006).
[34] J.-P. Wang, W. K. Shen, J. M. Bai, R. H. Victora, J. H. Judy, and W. L. Song, Appl. Phys. Lett. **86**, 142504 (2005).
[35] D. Suess, T. Schrefl, S. Fähler, M. Kirschner, G. Hrkac, F. Dorfbauer, and J. Fidler, Appl. Phys. Lett. **87**, 012504 (2005).
[36] N. F. Supper, D. T. Margulies, A. Moser, A. Berger, H. Do, and E. E. Fullerton, J. Appl. Phys. **99**, 08S310 (2006).
[37] D. Suess, Appl. Phys. Lett. **89**, 113105 (2006).
[38] E. Kneller, in *Handbuch der Physik XIII/2: Ferromagnetismus*, edited by H. P. J. Wijn (Springer, New York, 1966), p. 438.
[39] J. P. Liu, R. Skomski, Y. Liu, and D. J. Sellmyer, J. Appl. Phys. **87**, 6740 (2000).
[40] M. Zheng, R. Skomski, Y. Liu, and D. J. Sellmyer, J. Phys.: Condens. Matter **12**, L497 (2000).
[41] R. Skomski, J. Appl. Phys. **83**, 6724 (1998).